Micellation and gelation of block-copoly(oxyethylene/oxybutylene) in aqueous solutions

Micellization and Gelation of *block*-Copoly(oxyethylene/oxybutylene) in Aqueous Solution

Siriporn Tanodekaew, Nan-Jie Deng, Sibyl Smith, Yung-Wei Yang, David Attwood,* and **Colin Booth**

Manchester Polymer Centre, Departments of Chemistry and Pharmacy, University of Manchester, Manchester M13 9PL, U.K.

A series of diblock copolymers $E_{30}B_n$, with n in the range 3 to 16, was prepared by sequential anionic polymerization, and the association behavior of the copolymers in aqueous solution was investigated, as was the gelation of their concentrated micellar solutions. At temperatures in the range 30–50 °C, a minimum B-block length of four to five units was required for micellization. Gelation of micellar solutions of the copolymers was observed for copolymers with B-block lengths of six to seven units or more. The relationships between (i) standard Gibbs energy of micellization and molecular characteristics and (ii) critical gelation concentration and micellar characteristics were explored.

Introduction

The micellization and gelation of diblock and triblock copolymers of ethylene oxide and butylene oxide (E_mB_n and $E_mB_nE_m$, where E represents an oxyethylene unit and B an oxybutylene unit) in aqueous solution has been reported in recent publications from this laboratory.[1-5] By introducing a more hydrophobic chain unit, work on these systems extends that on corresponding properties of aqueous solutions of triblock copolymers of ethylene oxide and propylene oxide ($E_mP_nE_m$, where P represents an oxypropylene unit); see, e.g., refs 6–11. Equally importantly, the use of oxyethylene–oxybutylene block copolymers avoids certain problems related to sample purity and reproducibility which are either inherent in the polymerization of propylene oxide[12,13] or result from industrial preparative processes.[9]

As pointed out previously,[1,4] E_mB_n and $E_mB_nE_m$ copolymers in aqueous solution associate more readily than those $E_mP_nE_m$ copolymers of comparable E-content and overall chain length, consistent with the greater hydrophobicity of the B-block. Nevertheless, the micelles formed from the EB copolymers have similar molar masses and hydrodynamic radii to those characteristic of EP copolymers. As a consequence, gelation of concentrated micellar solutions of the E_mB_n and $E_mB_nE_m$ copolymers occurs in a similar region of the temperature–concentration diagram to that normally encountered for $E_mP_nE_m$ copolymers. This is consistent with a mechanism of gelation dominated by packing of micelles, with the gel–sol boundaries determined predominantly by micellar concentration and swelling.[3,5,9,10]

Previously[4,5] we have reported on the micellization in aqueous solution of six diblock copolymers ($E_{92}B_7$, $E_{50}B_{13}$, $E_{49}B_8$, $E_{50}B_4$, $E_{24}B_{10}$, and $E_{27}B_5$) and, in more detail, on the micellar properties and gelation of concentrated micellar solutions of three of the copolymers ($E_{50}B_{13}$, $E_{49}B_8$, and $E_{24}B_{10}$). The present paper describes work carried out on a range of E_mB_n copolymers all with similar E-block lengths (*ca.* E_{30}) and with B-block lengths covering a similar range as before, i.e. $E_{27}B_{16}$, $E_{29}B_{14}$, $E_{32}B_{10}$, $E_{30}B_8$, $E_{27}B_7$, $E_{28}B_5$, and $E_{32}B_3$. As described below, with the exception of copolymer $E_{32}B_3$, these copolymers associated in aqueous solutions, forming micelles of 10 or more chains at concentrations below 1 wt % copolymer and temperatures in the range 30–60 °C. The synthesis of the copolymers with short B blocks was directed toward better identification of the lower limits of micellization and gelation in E_mB_n copolymers.

Experimental Section

Materials. The copolymers were prepared by sequential anionic polymerization of ethylene oxide followed by butylene oxide.

Monofunctional chains were initiated by 2-(2-methoxyethoxy)-ethanol via its potassium salt. Vacuum line and ampule techniques were used throughout, in order to minimize initiation by moisture of unwanted difunctional chains. The methods used have been described in detail previously.[4]

The poly(oxyethylene) precursors (sampled after completion of the first stage of polymerization) and the final copolymers were all characterized by gel permeation chromatography (GPC) and ^{13}C NMR spectroscopy (see below for methods). The results are summarized in Table I. All GPC curves contained single narrow peaks which were analyzed to provide values of the molar mass corresponding to the elution volume at the peak (M_{pk}, calibration with poly(oxyethylene) standards) and measures of the width of the chain length distribution (ratio of weight-average to number-average molar mass, M_w/M_n). Values of M_n were obtained from ^{13}C NMR spectroscopy by end-group analysis together with copolymer compositions, the assignments being taken from previous work.[14]

As discussed previously,[4] possible impurities were triblock copolymers, from difunctional poly(oxyethylene) initiated by moisture in stage 1, and difunctional poly(oxybutylene) initiated by moisture in stage 2. These were assessed by quantitative assessment by NMR spectroscopy of proportions of the various end groups and the EB junctions.[4,14] It was found that moisture had been effectively excluded in the first stage of polymerization, but not in the second stage, leading to formation of a small proportion (<3 wt %) of poly(oxybutylene). Purification was effected either by adding hexane to a dilute solution of the copolymer in dichloromethane, which precipitated the copolymer and left the poly(oxybutylene) in solution, or by repeatedly extracting the polymer with warm hexane and separating the solid and liquid phases after cooling to *ca.* 10 °C. The evidence from dynamic light scattering, presented below, was that these procedures were effective in reducing the impurity level to well below 0.1 wt %.

The formulas of the copolymers given in the left-hand column of Table I were calculated from M_n of the poly(oxyethylene) block, determined by NMR after stage one of the synthesis, and the overall composition of the copolymer, determined by NMR after stage 2 and purification. The estimated uncertainties in the formulas are ±2 E units and ±1 B unit.

Cloud Point. Aqueous solutions of the copolymers in small test tubes were slowly heated (0.5 K min⁻¹) in a water bath to 100 °C and clouding (if any) was observed visually.

Light Scattering. Solutions for light scattering were generally clarified by filtering through Millipore filters (3 × 0.22-μm porosity, and one or more times 0.1-μm porosity) the final filtration being directly into the cleaned scattering cell. Refractive index

* Abstract published in *Advance ACS Abstracts*, October 15, 1993.

TABLE I: Molecular Characteristics of the E_mB_n Block Copolymers

overall formula	M_{pk}/g mol^{-1} (GPC)	M_w/M_n (GPC)	M_n/g mol^{-1} (NMR)	mol % E (NMR)	wt % E (NMR)
$E_{27}B_{16}$	2520	1.09	2340	62.8	50.8
$E_{29}B_{14}$	3210	1.07	2280	67.4	55.9
$E_{32}B_{10}$	2150	1.06	2130	76.2	66.1
$E_{30}B_8$	2450	1.07	1900	79.0	69.6
$E_{27}B_7$	1690	1.05	1690	79.4	70.2
$E_{28}B_5$	2050	1.07	1590	84.9	77.4
$E_{32}B_3$	1530	1.04	1620	91.4	86.7

increments were estimated from previous results and checked by means of an Abbé 60/ED precision refractometer (Bellingham and Stanley).

Static light scattering intensity measurements were made by means of a Malvern PCS100 instrument with vertically polarized incident light of wavelength 488 nm supplied by an argon-ion laser (Coherent Innova 90) operated at 500 mW or less. The intensity scale was calibrated against benzene. Measurements were made at angles of 45°, 90°, and 135° to the incident beam. In an experiment, measurements were made either on solutions at a given temperature over a range of concentration (to determine the micellar molar mass) or on solutions of given concentration over a range of temperature (to determine the critical micelle temperature). In the latter case, the temperature of the scattering cell was raised or lowered at *ca.* 1 K min^{-1}.

The temperature dependence of the intensity of scattered light was also determined by means of a modified Sofica instrument with unpolarized light of wavelength 633 nm supplied by a 5-mW stabilized helium–neon laser (Uniphase Model 1122). For purposes of comparison with results obtained by using the other instrument, scattering intensities were calibrated against scattering from benzene *via* a secondary glass standard.

Dynamic light scattering measurements were made by means of the Malvern instrument described above combined with a Malvern K7027 autocorrelator using 60 linearly-spaced channels with a far-point delay of 1024 sample times. Measurements of scattered light were made at an angle of 90° to the incident beam. The data were analyzed either by the CONTIN method, thus gaining information on the distribution of decay rates, or, if appropriate, by a single exponential fit of the correlation curve.

Gelation. The gel–sol behavior of concentrated aqueous solutions of the diblock copolymers was investigated as follows. A solution of the block copolymer was enclosed in a small tube and observed on heating from –15 to 80 °C and the change from a mobile to an immobile system (or vice versa) was determined by inverting the tube. The method served to define the sol–gel transition temperatures to about ±1 K. When checked, the stiff gels were found to be immobile in the inverted tubes over time periods of weeks. Separation of water from the gel (syneresis) was often observed toward the high-temperature limit of the gel region; otherwise the systems were homogeneous.

Results and Discussion

Cloud Points. The 1 wt % solutions of copolymers $E_{30}B_{10}$, $E_{27}B_7$, $E_{28}B_5$, and $E_{32}B_3$ were clear as prepared at room temperature and clouding was not detected below 100 °C. A 1 wt % solution of copolymer $E_{27}B_{16}$ was cloudy as prepared at room temperature and became markedly more cloudy at *ca.* 60 °C. However, a 1 wt % solution prepared at 2 °C was clear and remained clear as the temperature was raised, finally clouding at *ca.* 60 °C. This feature of the solution of copolymer $E_{27}B_{16}$, consistent with formation of a molecular solution from the solid copolymer only in a very good solvent, was not investigated further.

Dynamic Light Scattering. Light scattering measurements were restricted to temperatures below 60 °C. Solutions in the concentration range 4–100 g dm^{-3} were studied by dynamic light scattering. The results, analyzed by the constrained regularization
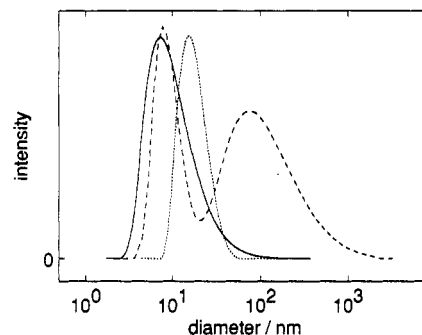

Figure 1. Dynamic light scattering intensity (arbitrary scale, curves adjusted to approximately the same maximum value) versus logarithm of particle diameter for aqueous solutions of E_mB_n copolymers: (···) $E_{32}B_{10}$, 1.8 g dm^{-3}, 35 °C, normal filtration; (– – –) $E_{27}B_7$, 10 g dm^{-3}, 30 °C, 3 × 0.22-μm filter only; (——) $E_{27}B_7$, 7 g dm^{-3}, 35 °C, additional filtration through 0.10-μm filter. Note that the intense scattering from the large particles (diameter ≈ 100 nm) in the coarsely filtered solution of copolymer $E_{27}B_7$ derives from only *ca.* 0.03 wt % of the sample.
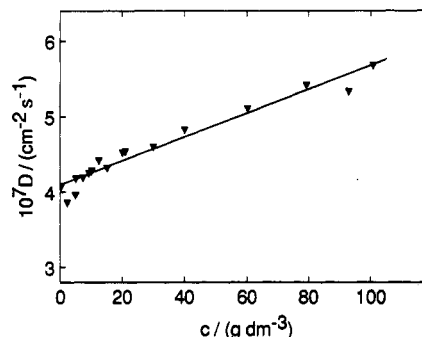

Figure 2. Diffusion coefficient from dynamic light scattering (D) versus concentration for aqueous solutions of block copolymer $E_{30}B_8$ at 30 °C.

CONTIN technique developed by Provencher,[15] served to confirm the presence of micelles and also to determine micellar size. For well-filtered solutions, the decay rate distribution, $G(\tau)$, contained a narrow peak centered on a fast decay rate; see Figure 1. Solutions of copolymer $E_{27}B_{16}$ prepared at low temperature followed this general pattern. The exception was copolymer $E_{32}B_3$, aqueous solutions of which showed no evidence of micellization under the conditions investigated.

A brief investigation of clarification procedures was undertaken. It was found that certain copolymer solutions when filtered repeatedly through 0.22-μm filters still contained a small proportion (estimated to be ≪0.1 wt %) of large particles, which gave rise to significant scattering; see Figure 1. However, this material was effectively removed by filtration through the 0.1-μm filter (see Figure 1), much as described previously[6] by Zhou and Chu for Pluronic L64. As described below, evidence of an extremely small proportion of insoluble material in the form of large particles was evident in static light scattering from very dilute solutions of copolymer $E_{28}B_5$. A limit to the degree of purification achieved by precipitation/extraction methods, particularly when used in conjunction with coarse filtration, was recognized during the investigation, and precautions were taken to minimize any effects. In particular, the contribution of impurities to scattering intensities for well-filtered solutions of moderate concentration (20–100 g dm^{-3}) was judged to be insignificant, and data were generally extrapolated to infinite dilution from this concentration range.

The average decay rates obtained for the micellar peaks were transformed to average diffusion coefficients, D. Where appropriate, average values of D were also determined from a single-exponential fit of the correlation curve. The concentration dependence of D was investigated for micellar solutions of copolymer $E_{30}B_8$ in solution at 30 °C; see Figure 2. Similar concentration dependences have been found for micellar solutions

TABLE II: Micellization of the E_mB_n Block Copolymers in Aqueous Solution[a]

copolymer	$T/°C$	r_h/nm	$M_w/10^4$ g mol^{-1}	N_w	r_t/nm
$E_{27}B_{16}$	30	9[b]			
$E_{29}B_{14}$	30		35	140	7.2
$E_{32}B_{10}$	30	7[b]	13	60	5.2
	50		17	74	5.6
$E_{30}B_8$	30	7	12	60	5.1
$E_{27}B_7$	30		2.8	16	2.5
	45	5[b]			
	50		7.2	42	3.7
	57	5[b]			
$E_{28}B_5$	30	5[b]	1.6	10	2.0

[a] Estimated uncertainties: r_h, M_w, and N_w, ±10%; r_t, ±5%. [b] Apparent values of r_h estimated from measured diffusion coefficients of micelles in dilute solution.
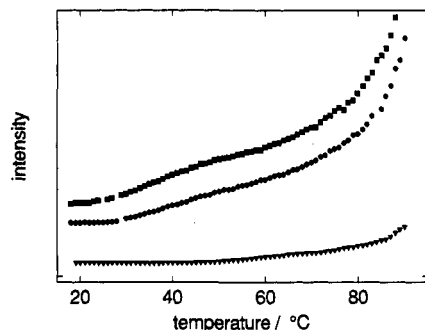

Figure 3. Light scattering intensity (arbitrary scales and zeros) versus temperature for aqueous solutions of block copolymer $E_{27}B_7$: (■) 1 g kg^{-1}; (●) 0.79 g kg^{-1}; (▼) 0.28 g kg^{-1}.

of related copolymers.[4] Within the experimental scatter, the values of D can be linearly extrapolated to $c = 0$ to obtain a value of the micellar translational diffusion coefficient, D_0. Application of the Stokes–Einstein equation gave the micellar hydrodynamic radius (r_h, radius of the hydrodynamically-equivalent hard sphere)

$$r_h = kT/(6\pi\eta D_0) \qquad (1)$$

where k is the Boltzmann constant and η is the viscosity of water at temperature T. A value of $r_h = 7$ nm was obtained, as listed in Table II. The concentration dependence of D was not determined for the other copolymers. Apparent values of r_h (see Table II), estimated from the measured diffusion coefficients of micelles in solutions of various dilute concentrations, serve as approximate guides to hydrodynamic dimensions.

Critical Micelle Temperature. Plots of static light scattering intensity versus temperature were obtained for aqueous solutions of copolymers $E_{27}B_7$ and $E_{28}B_5$; representative curves are shown in Figure 3. The temperature at which a scattering curve left the baseline was assumed to indicate the onset of micellization, i.e. the critical micellization temperature (cmT). The results of dynamic light scattering, described above, served to confirm that the effect was due to micellization. As discussed further below, an appropriate plot of the results is $\log_{10} c$ versus inverse critical micelle temperature; see Figure 4. Within the experimental scatter, the results for the two copolymers cannot be distinguished.

Aqueous solutions of copolymers $E_{30}B_8$, $E_{32}B_{10}$, $E_{29}B_{14}$, and $E_{27}B_{16}$ could not be investigated in this way, as the critical micellization temperatures of solutions of these copolymers of sufficient concentration (i.e. $c > 1$ g dm^{-3}) to allow reliable detection of light scattering intensity were below the lower temperature limit of our apparatus ($T \approx 15$ °C).

Micellar Molar Mass. The plot of $\log_{10} c$ versus $1/(cmT)$ shown in Figure 4 can equally well be regarded as a plot of $\log_{10}$-(cmc) versus $1/T$, where cmc is the critical micelle concentration at temperature T. As can be seen, aqueous solutions of copolymers $E_{27}B_7$ and $E_{28}B_5$ have fairly high values of the cmc at low temperatures, e.g. about 6 g dm^{-3} at 30 °C. Consequently,
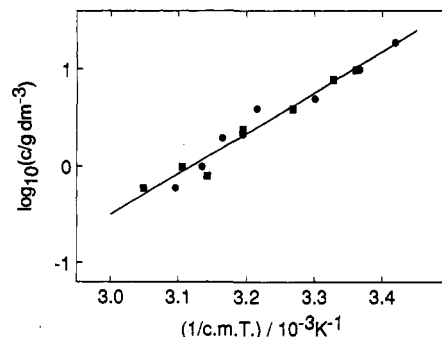
Figure 4. $\log_{10} c$ versus $1000/cmT$ for aqueous solutions of copolymers (■) $E_{27}B_7$ and (●) $E_{28}B_5$.
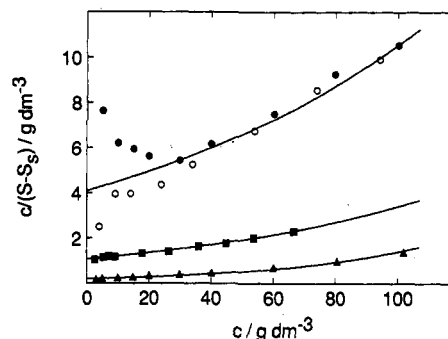
Figure 5. Scattering function $c/(S - S_s)$ versus c for aqueous solutions of (●) $E_{28}B_5$, 30 °C, (■) $E_{27}B_7$, 50 °C, and (▲) $E_{29}B_{14}$, 30 °C. Unfilled symbols (O) are for scattering function $(c - cmc)/(S - S_s)$ versus $(c - cmc)$ for aqueous solutions of $E_{28}B_5$ at 30 °C: cmc = 6 g dm^{-3}. The curves are calculated from eqs 2 and 3 as described in the text.

solutions of those copolymers at low temperatures became predominantly micellar only at moderate to high concentrations. This is illustrated in Figure 5, in which the scattering function $c/(S - S_s)$ is plotted against c for aqueous solutions of copolymer $E_{28}B_5$ at 30 °C, S being the intensity of light scattered from solution relative to that scattered from benzene and S_s being the corresponding quantity for light scattered from solvent (pure water). The upturn at low concentrations ($c < 30$ g dm^{-3}) is a result of micellar dissociation. Values of $c/(S - S_s)$ below the cmc should correspond to unassociated copolymer molecules, i.e. *ca.* 40 g dm^{-3} for copolymer $E_{28}B_5$. The measured values were about one-quarter of the expected values (see Figure 5) indicative (as discussed above) of a very small proportion of impurities in the form of large particles. The evidence from dynamic light scattering (see above) was that scattering from well-filtered solutions of concentration above 40 g dm^{-3} was predominantly from micelles, with insignificant contribution from impurities. The curvature of the scattering function in the moderate concentration range is caused by interference of light scattered from neighboring micelles.

The micellar concentration can be approximated by deducting the cmc from the overall total copolymer concentration, in which case the scattering function $(c-cmc)/(S - S_s)$ is plotted against $(c-cmc)$; see Figure 5. The correction is significant at concentrations below $c = 30$ g dm^{-3} but less significant at higher concentrations where micelles are predominant. A similar correction was made to the scattering data for solutions of copolymer $E_{27}B_7$ at 30 °C. Corresponding plots for aqueous solutions of copolymer $E_{27}B_7$ at 50 °C and $E_{29}B_{14}$ at 30 °C, in which micellization occurred at low concentrations, were little affected by micellar dissociation; see Figure 5.

Whether or not correction was made for micellar dissociation, the extrapolation to zero concentration to obtain the micellar molar mass was curved. Within the concentration range where micellization was essentially complete, measurements of scattering intensities at 45° and 135° confirmed that the dissymmetry (Z

$= S_{45}/S_{135}$) was $Z \approx 1$, i.e. that scattering was from small particles. Assuming spherical micelles, interparticle interference was accounted for by scattering theory for hard spheres. A satisfactory extrapolation procedure was based on the Carnahan–Starling equation,[16] as discussed previously in its application to micellar solutions of E_mB_n and $E_mB_nE_m$ copolymers.[1-4] The equation is

$$K^*c/(S - S_s) \sim 1/QM_w \tag{2}$$

where Q is the interparticle scattering factor (the intraparticle scattering factor being unity for small micelles), c is the concentration of micelles, and M_w is the weight-average molar mass of the micelles. Q is given by

$$1/Q = [(1 + 2\phi)^2 - \phi^2(4\phi - \phi^2)](1 - \phi)^{-4} \tag{3}$$

where ϕ is the volume fraction of equivalent thermodynamic uniform spheres, which can be calculated from the actual volume fraction of copolymer in micelles in the system by applying a volume swelling factor (δ_t = swollen volume relative to dry volume). Concentration c was equated to (c – cmc) when appropriate. The adjustable parameters were M_w and δ_t.

In order to apply the method, the refractive index increment was estimated from previous[1,2,4] and present results for aqueous solutions of E_mB_n and $E_mB_nE_m$ copolymers in the composition range 0–50 wt % B. Within a spread of ±0.004 cm³ g⁻¹, values of dn/dc were constant across the composition range at 0.138 cm³ g⁻¹, with a temperature derivative of approximately -2×10^{-4} cm³ g⁻¹ K⁻¹. Concentrations were converted to a volume basis assuming a density of dry polymer of $\rho = 1.07$ g dm⁻³, irrespective of composition.

Extrapolations from the moderate concentration range minimized any effects of incomplete clarification (see above), but the relatively short range over which the data were fitted made the values of M_w and δ_t for solutions of copolymers $E_{28}B_5$ and $E_{27}B_7$ uncertain. Fits were obtained with greater certainty for solutions of $E_{27}B_7$ at 50 °C and for solutions of the other copolymers with longer B blocks at all temperatures in the range considered (see Figure 5). Values of M_w and thermodynamic radius

$$r_t = (3\delta_t M_w/4\pi N_A \rho)^{1/3} \tag{4}$$

obtained for the micelles are listed in Table II. The association numbers of the micelles (see Table II) were calculated from

$$N_w = M_w(\text{micelle})/M_w(\text{molecule}) \tag{5}$$

where M_w(molecule) was obtained from the values of M_n and M_w/M_n listed in Table I.

Within the series of copolymers with similar E-block lengths (E_{30}) the association numbers of the micelles at a given temperature (e.g. 30 °C) increased as the B-block length was increased in the range B_5 to B_{14}. As found for other systems (see, e.g., ref 4) the association numbers and thermodynamic dimensions (r_t) of the micelles increased with temperature. It has been established for many copolymer systems, including related E_mB_n copolymers,[4] that hydrodynamic radii (r_h) are approximately independent of temperature. The present results for micelles of copolymer $E_{27}B_7$ are consistent with this. The difference in physical origin between the two measures of micellar size is important: the hydrodynamic radius mainly reflects the size of the non-free-draining fringe, whereas the thermodynamic radius mainly reflects the excluded volume of the fringe. Overall, the present and previous results indicate that the excluded volume is more sensitive to temperature than is the hydrodynamic volume.

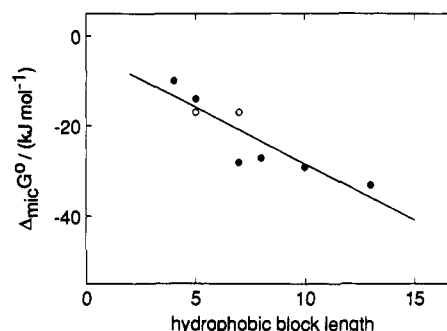**Thermodynamics of Micellization.** For association to be conveniently detectable by light scattering, the equilibrium

Figure 6. Standard Gibbs energy of micellization, $\Delta_{mic}G^\circ$, vs hydrophobic block length (n) for aqueous solutions of diblock copolymers (E_mB_n): (O) present results; (●) previous[4] results.

between molecules (A) and micelles (A_N) of association number N

$$A \rightleftharpoons (1/N)A_N \tag{6}$$

must be characterized by large values of N and equilibrium constant (K). Under these circumstances, values of the standard Gibbs energy of micellization ($\Delta_{mic}G^\circ$) can be conveniently determined[17] from the approximate relationship

$$\Delta_{mic}G^\circ \approx RT \ln(\text{cmc}) \tag{7}$$

This Gibbs energy change refers to standard states of copolymer chains in ideally dilute solution at unit concentration (1 mol dm⁻³) and copolymer chains in the micellar state. The temperature dependence of the cmc gives the standard enthalpy of micellization from

$$\Delta_{mic}H^\circ \approx R\{d \ln(\text{cmc})/d(1/T)\} \tag{8}$$

and thereby the standard entropy of micellization $\Delta_{mic}S^\circ$. In terms of the cmT, eqs 7 and 8 become

$$\Delta_{mic}G^\circ \approx R(\text{cmT}) \ln c \tag{9}$$

and

$$\Delta_{mic}H^\circ \approx R\{d \ln c/d[1/(\text{cmT})]\} \tag{10}$$

For copolymers $E_{28}B_5$ and $E_{27}B_7$, averaging *via* the straight line shown in Figure 4, the value of the Gibbs energy of micellization at 40 °C is $\Delta_{mic}G^\circ \approx -17 \pm 1$ kJ mol⁻¹. The standard enthalpy of micellization from the slope of the straight line is $\Delta_{mic}H^\circ \approx +80 \pm 10$ kJ mol⁻¹, and the corresponding contribution of the standard entropy of micellization to $\Delta_{mic}G^\circ$ is $-T\Delta_{mic}S^\circ \approx -97 \pm 10$ kJ mol⁻¹. As usual for micellization of block copolymers in aqueous solution, the standard entropy change is positive. Values of N obtained for the two copolymers were in the range 10–36; see Table II. Even at the low end of the range, the error introduced into the determination of K by setting the value of $[A_N]^{1/N} = 1$ is only *ca.* 1%, and the corresponding errors in $\Delta_{mic}G^\circ$ and $\Delta_{mic}H^\circ$, which depend on ln K and its temperature derivative, are insignificant.

The two values of $\Delta_{mic}G^\circ$ at 40 °C which were obtained in the present work are compared with values obtained previously[4] for E_mB_m copolymers *via* surface tension measurements in Figure 6, where $\Delta_{mic}G^\circ$ is plotted against B-block length irrespective of E-block length. Agreement between the two sets of results is satisfactory, and the complete set of results shows a useful approximate correlation of $\Delta_{mic}G^\circ$ with hydrophobic block length.

Values of $\Delta_{mic}H^\circ$ reported previously[1,3,4] for aqueous solutions of $E_{24}B_{10}$, $E_{40}B_{15}E_{40}$, and $E_{58}B_{17}E_{58}$ are lower than the present value, i.e. $\Delta_{mic}H^\circ \approx +30$–40 kJ mol⁻¹, although the oxybutylene block lengths are longer. These previous results were obtained by determination of the cmc at various temperatures by extrapolation of light scattering intensities measured for solutions of
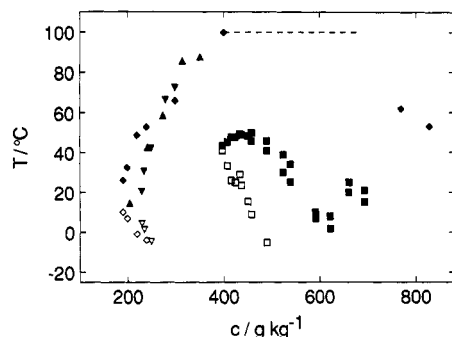
Figure 7. Gel–sol diagram for aqueous micellar solutions of copolymers: ($\blacksquare$, $\square$) $E_{27}B_7$; ($\blacktriangledown$, $\triangledown$) $E_{30}B_8$; ($\blacklozenge$, $\lozenge$) $E_{32}B_{10}$; ($\blacktriangle$) $E_{27}B_{16}$. Unfilled symbols denote sol → gel transition on heating; filled symbols denote gel → sol transition on heating. The dashed line indicates solutions of copolymer $E_{32}B_{10}$ which were gels below 100 °C.

Figure 8. Critical concentration for gel formation (cgc) versus M_w/r_t^3 for aqueous micellar solutions of ($\bullet$, $\circ$) diblock and ($\blacksquare$) triblock copolymers. Unfilled symbols represent results from present work and filled symbols from previous work.[5]

different concentrations back to the value characteristic of a molecular solution. Values obtained[4] for the cmc by surface tension measurements for solutions of copolymer $E_{50}B_{13}$ at 20 and 40 °C are consistent with a low value of $\Delta_{mic}H^\circ$. While all methods are valid, determination of the cmT is most direct and, for that reason, the cmT method is more reliable. Unfortunately, as pointed out above, because of the low scattering intensities involved, the cmT method could not be used when the cmc was low. It is possible that the difference in behavior originates from the longer oxybutylene blocks being more tightly coiled in the molecular state in aqueous solution, so that interaction with water molecules via hydrophobic bonding is much reduced compared with that prevailing for the shorter blocks. So far as Gibbs energy is concerned, it is clear from Figure 6 that the larger enthalpy of micellization is compensated by a larger entropy of micellization, as might be expected for the hydrophobic effect.[18]

Considering the micellization of $E_mP_nE_m$ copolymers in dilute aqueous solution, and taking a particular example, $E_{93}P_{44}E_{93}$ (Synperonic F127), a value of $\Delta_{mic}H^\circ \approx +300$ kJ mol^{-1} has been reported,[9] i.e. ca. 7 kJ (mol P-units)$^{-1}$. The present results for copolymers $E_{28}B_5$ and $E_{27}B_7$ (taking an average chain length) indicate ca. 13 kJ (mol B-units)$^{-1}$, consistent with a more hydrophobic unit.

Gelation. The results available from previous[4] and present studies, described above, show that the lower limit for micellization in E_mB_n copolymers of the type under discussion is an oxybutylene block length of 4 units. While micellization is a necessary preliminary to gelation in these systems, it is not in itself sufficient. Considering solutions of spherical micelles, the conditions for gelation depend critically on micellar concentration and micellar size.[5] Changes in micellar shape (e.g. spherical → cylindrical) introduce other considerations.[11] Accordingly, the present study was extended to include the gelation of concentrated solutions of the copolymers.

Gelation was not observed for solutions of copolymers $E_{32}B_3$ and $E_{28}B_5$, observations being made on solutions up to 75 wt % copolymer concentration over the temperature range 0–80 °C. The negative result for copolymer $E_{32}B_3$ was expected, as this copolymer did not micellize. That for copolymer $E_{28}B_5$ is a consequence of the small size of the micelles. Results for other copolymer solutions are summarized in the gel–sol diagram shown in Figure 7. Separation of water from the gel (syneresis) was generally observed at a temperature a little below the high-temperature gel–sol boundary. Interestingly, the critical conditions for gelation of micellar solutions of copolymers $E_{30}B_8$, $E_{32}B_{10}$, and $E_{27}B_{16}$ are similar; see Figure 7. This is to be understood in terms of micellar size and concentration, as discussed below.

If gelation results from close packing of micelles acting effectively as hard spheres, then the critical gelation concentration
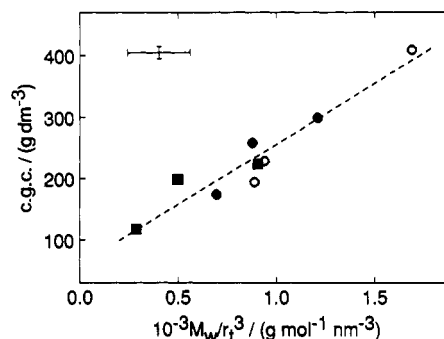
(cgc in g dm^{-3}) is given by

$$\text{cgc} = (2^{1/2}/8r_{hs}^3)(10^{24}M/N_A) = 0.292M/r_{hs}^3 \quad (11)$$

where r_{hs} is the equivalent hard-sphere radius in nm and M is the molar micellar mass in g mol^{-1}. Molecular weights (M_w) and thermodynamic radii (r_t) determined by static light scattering for micelles of the present copolymers in aqueous solutions of moderate concentration are listed in Table II. Assuming that M and r_{hs} can be related directly to M_w and r_t, observed values of the cgc are plotted against M_w/r_t^3 in Figure 8, which includes results from previous work. Given the experimental error in M_w/r_t^3 (see Figure 8) the correlation of experiment with expectation is very satisfactory.

No result for copolymer $E_{27}B_{16}$ is included in Figure 8, as the micelles of this copolymer were not characterized by static light scattering. Given the values of the cgc found for the micellar solutions of copolymer $E_{27}B_{16}$, and the correlation of Figure 8, it can be inferred that the value of the ratio M/r_t^3 for micelles of this copolymer in aqueous solution at $T \approx 30$ °C lies in the range 800–1000 g mol^{-1} nm^{-3}. In this respect, it is satisfactory that static light scattering results for solutions of the related copolymer $E_{29}B_{14}$ (see Table II) yield a value of $M/r_t^3 \approx 950$ g mol^{-1} nm^{-3}.

The upper gel–sol transition temperatures of aqueous micellar solutions of copolymer $E_{27}B_7$ are reduced as concentration is increased in the high concentration range, i.e. $c > 450$ g kg^{-1}. Evidence of a similar effect was sought for solutions of copolymer $E_{32}B_{10}$. For that system, the upper gel–sol boundary in the concentration range $c = 550$–700 was not observed, as it lay outside the range of our experiments at $T > 100$ °C. However gel–sol transitions were observed at 62 and 53 °C for solutions of very high concentration ($c \approx 770$ and 828 g kg^{-1}, respectively, see Figure 6). This behavior, whereby it is possible to pass through the gel region (i.e. sol → gel → sol) by changing the concentration at constant temperature, must be a consequence of a changed micellar structure at high concentration. Changes in micellar structure from spherical to cylindrical or lamellar as concentration is increased are well documented (see, e.g. refs 17 and 18) and have been demonstrated in concentrated solutions of triblock oxyethylene–oxypropylene ($E_mP_nE_m$) copolymers.[11] The structures of the present gels have not been investigated.

References and Notes

(1) Luo, Y.-Z.; Nicholas, C. V.; Attwood, D.; Collett, J. H.; Price, C.; Booth, C. *Colloid Polym. Sci.* **1992**, *270*, 1094.

(2) Nicholas, C. V.; Luo, Y.-Z.; Deng, N.-J.; Attwood, D.; Collett, J. H.; Price, C.; Booth, C. *Polymer* **1993**, *34*, 138.

(3) Luo, Y.-Z.; Nicholas, C. V.; Attwood, D.; Collett, J. H.; Price, C.; Booth, C.; Zhou, Z.-K.; Chu, B. *J. Chem. Soc., Faraday Trans.* **1993**, *88*, 539.

(4) Bedells, A. D.; Arafeh, R. M.; Yang, Z.; Attwood, D.; Heatley, F.; Padget, J. C.; Price, C.; Booth, C. *J. Chem. Soc., Faraday Trans.* **1993**, *89*, 1235.

(5) Bedells, A. D.; Arafeh, R. M.; Yang, Z.; Attwood, D.; Padget, J. C.; Price, C.; Booth, C. *J. Chem. Soc., Faraday Trans.* **1993**, *89*, 1243.

(6) Zhou, Z.-K.; Chu, B. *Macromolecules* **1988**, *21*, 2548.

(7) Wanka, G.; Hoffmann, H.; Ulbricht, W. *Colloid Polym. Sci.* **1990**, *268*, 101.

(8) Brown, W.; Schillen, K.; Almgren, M.; Hvidt, S.; Bahadur, P. *J. Phys. Chem.* **1991**, *95*, 1850.

(9) Yu, G.-E.; Deng, Y.-L.; Dalton, S.; Wang, Q.-G.; Attwood, D.; Price, C.; Booth, C. *J. Chem. Soc., Faraday Trans.* **1992**, *88*, 2537.

(10) Malmsten, M.; Lindman, B. *Macromolecules* **1992**, *25*, 5440.

(11) Mortenson, K. *Macromolecules* **1993**, *26*, 805.

(12) Ding, J.-F.; Heatley, F.; Price, C.; Booth, C. *Eur. Polym. J.* **1991**, *27*, 895.

(13) Yang, L.; Bedells, A. D.; Attwood, D.; Booth, C. *J. Chem. Soc., Faraday Trans.* **1992**, *88*, 1447.

(14) Heatley, F.; Yu, G. E.; Sun, W. B.; Pywell, E. J.; Mobbs, R. H.; Booth, C. *Eur. Polym. J.* **1990**, *26*, 583.

(15) Provencher, S. W. *Makromol. Chem.* **1979**, *180*, 201.

(16) Carnahan, N. F.; Starling, K. E. *J. Chem. Phys.* **1969**, *51*, 635.

(17) Attwood, D.; Florence, A. T. *Surfactant Systems*; Chapman and Hall: London, 1982; p 473.

(18) Tanford, C. H. *The Hydrophobic Effect*; Wiley-Interscience: New York, 1973.